

Scandium-Promoted Direct Conversion of Dinitrogen into Hydrazine Derivatives via N–C Bond Formation

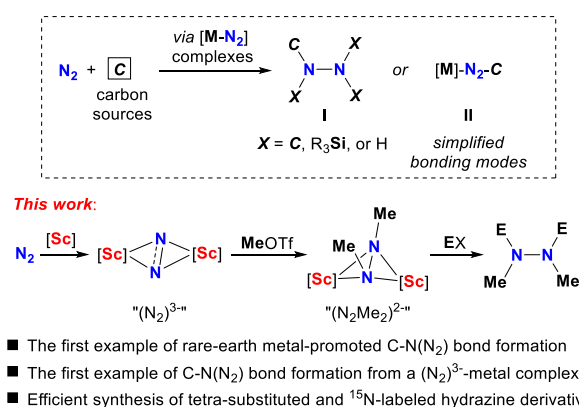
Ze-Jie Lv,^{1b} Zhe Huang,^{1b} Wen-Xiong Zhang,^{*1b} and Zhenfeng Xi^{*1b}

Beijing National Laboratory for Molecular Sciences (BNLMS), Key Laboratory of Bioorganic Chemistry and Molecular Engineering of Ministry of Education, College of Chemistry, Peking University, Beijing 100871, China

S Supporting Information

ABSTRACT: Direct conversion of dinitrogen (N_2) into organic compounds, not through ammonia (NH_3), is of great significance both fundamentally and practically. Here we report a highly efficient scandium-mediated synthetic cycle affording hydrazine derivatives ($RMeN-NMeR'$) directly from N_2 and carbon-based electrophiles. The cycle includes three main steps: (i) reduction of a halogen-bridged discandium complex under N_2 leading to a $(N_2)^{3-}$ -bridged discandium complex via a $(N_2)^{2-}$ -intermediate; (ii) treatment of the $(N_2)^{3-}$ complex with methyl triflate ($MeOTf$), affording a $(N_2Me_2)^{2-}$ -bridged discandium complex; and (iii) further reaction of the $(N_2Me_2)^{2-}$ complex with the carbon-based electrophile, producing the hydrazine derivative and regenerating the halide precursor. Furthermore, insertion of a CO molecule into one Sc–N bond in the $(N_2Me_2)^{2-}$ -scandium complex was observed. Most notably, this is the first example of rare-earth metal-promoted direct conversion of N_2 to organic compounds; the formation of C–N bonds by the reaction of these $(N_2)^{3-}$ and $(N_2Me_2)^{2-}$ complexes with electrophiles represents the first case among all N_2 -metal complexes reported.

Scheme 1. Metal-Promoted Synthesis of Hydrazine Derivatives Directly from N_2 via C–N Bond Formation



Most N-containing organic compounds are currently synthesized through ammonia (NH_3), the product of the Haber–Bosch process that converts N_2 and H_2 to NH_3 using metal catalysts under high temperature and pressure. Direct conversion of N_2 into high-value N-containing organic compounds, not through NH_3 , is of great significance and challenging both fundamentally and practically.¹ Although some progress in making C–N bonds through N_2 -transition metal^{2–4} or N_2 -actinide⁵ complexes and carbon-based reagents have been reported in the literature, such an approach is still in its infancy. As a class of important synthetic intermediates, hydrazine derivatives,⁶ which may contain up to four C–N bonds on the N–N single-bond skeleton, are primary targets for direct conversion of N_2 (Scheme 1).⁷ However, as far as we are aware, there are only a few examples of the direct use of N_2 as the nitrogen source for the construction of C–N bonds of hydrazine derivatives, affording either pure organic compounds (I)⁷ or hydrazido–metal complexes (II)⁸ as the final products (Scheme 1). Type I compounds have been realized via N_2 -metal complexes of Ti,^{7g} Zr,^{7e} Hf,^{7d,f} Mo,^{7a} and W,^{7b,c} while type II compounds have been made and structurally characterized via N_2 -metal

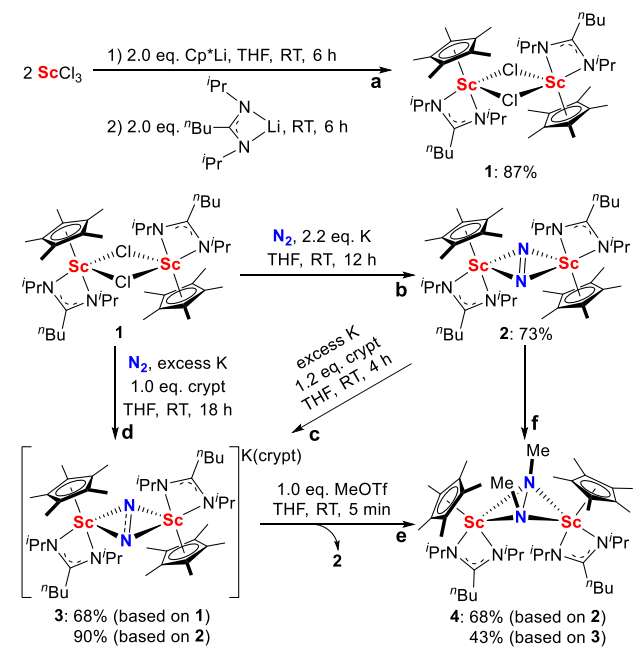
complexes of Ti,^{7g} Zr,^{8b} Hf,^{8c,d} Ta,^{8a,e} Mo,^{7a,b} and W.^{7b,c} Despite these advances, the efficiency of the transformation from N_2 to I or II and the diversity of transformation strategies in terms of metals used are still very limited.

In contrast to transition metals mentioned above, rare-earth metal-mediated conversion of N_2 to N-containing organic compounds has not yet been reported, even though more than 40 N_2 -rare-earth metal complexes have been documented by Evans and others.^{9,10} The absence of this chemistry is mainly due to the weakly activated N_2 ligand.^{11,12} Herein we report a highly efficient scandium-mediated route that affords hydrazine derivatives ($RMeN-NMeR'$) directly from N_2 and carbon-based electrophiles (Scheme 1). In this process, the $(N_2)^{2-}$, $(N_2)^{3-}$, and $(N_2Me_2)^{2-}$ -bridged discandium intermediates were isolated and structurally characterized. Furthermore, insertion of one CO molecule into a Sc–N bond of the $(N_2Me_2)^{2-}$ -scandium complex was achieved. To our knowledge, this is the first conversion of a $(N_2)^{3-}$ -metal complex to N-containing organic compounds among all metals over the periodic table. In addition, the formation of four C–N bonds on the N–N single-bond skeleton and ^{15}N -labeled hydrazine derivatives directly using N_2 or $^{15}N_2$ as the nitrogen source is also unprecedented.

The chloride-bridged discandium complex **1** could be easily prepared in a one-pot reaction from $ScCl_3$, Cp^*Li ($Cp^* = C_5Me_5$), and $Li[{}^nBuC(N^iPr)_2]$ in 87% yield (Scheme 2a). When **1** was treated with 2.2 equiv of potassium under N_2 in

Received: April 21, 2019

Scheme 2. Synthesis of Complexes 1–4



THF, the $(\text{N}_2)^{2-}$ -bridged discandium complex **2** was obtained in 73% yield (Scheme 2b). The ^{15}N analogue ^{15}N -**2** was prepared from $^{15}\text{N}_2$ by a similar procedure. X-ray analysis of **2** revealed a dinuclear structure with a side-on bridging $(\text{N}_2)^{2-}$ ligand (Figure S27). The Sc_2N_2 skeleton of **2** is similar to the $(\text{N}_2)^{2-}$ -Sc complex $[(\text{C}_5\text{Me}_5\text{H})_2\text{Sc}]_2(\mu\text{-}\eta^2\text{:}\eta^2\text{-N}_2)^{9f}$ with a comparable N–N bond length. The Raman spectrum of **2** exhibits a strong absorption at 1420 cm^{-1} assignable to the N–N stretch.¹³ On the basis of the $^{15}\text{N}/^{14}\text{N}$ mass ratio, the absorption in the ^{15}N -**2** Raman spectrum shifts to 1371 cm^{-1} . In the ^{15}N NMR spectrum of ^{15}N -**2**, the $(^{15}\text{N}_2)^{2-}$ ligand displays a chemical shift at 455.90 ppm, higher than that observed for $[(\text{C}_5\text{Me}_5\text{H})_2\text{Sc}]_2(\mu\text{-}\eta^2\text{:}\eta^2\text{-N}_2)$ (385 ppm).^{9f}

Sc-mediated N_2 activation is experimentally more challenging than with other rare-earth metals because of the small size and electropositive nature of scandium.⁹ The first side-on-bridged $(\text{N}_2)^{2-}$ -Sc complex was prepared by reduction of the cationic precursor $[(\text{C}_5\text{Me}_5\text{H})_2\text{Sc}][(\mu\text{-Ph})\text{BPh}_3]$ with KC_8 under N_2 ^{9f} or by the direct reaction of $[(\text{C}_5\text{Me}_5\text{H})_3\text{Sc}]$ with N_2 .^{9g} Recently, an end-on-bridged $(\text{N}_2)^{2-}$ -Sc complex was prepared via the reduction of $\text{Sc}[\text{N}(\text{SiMe}_3)_2]_3$ under N_2 .¹⁴ The transformation from **1** to **2** provides for the first time a convenient route to obtain rare-earth metal– N_2 complexes directly from the chloride precursors.

When **2** was treated with potassium in the presence of [2.2.2]cryptand (crypt) at room temperature, the paramagnetic $(\text{N}_2)^{3-}$ -bridged discandium complex **3** was isolated in 90% yield (Scheme 2c). **3** could also be prepared directly in 68% yield via in situ generation of **2** from **1** (Scheme 2d). X-ray analysis revealed that **3** is a separated ion pair in which the whole $(\text{Sc}_2\text{N}_2)^-$ anion is balanced by a potassium crypt ion (Figure 1). The Sc_2N_2 unit in **3** is planar, and the dinitrogen ligand adopts a side-on $\mu\text{-}\eta^2\text{:}\eta^2\text{-N}_2$ mode. The N–N bond length is 1.3963(16) Å, which is between the lengths of a N=N double bond (1.25 Å for PhNNPh) and a N–N single bond (1.46 Å for H_2NNH_2) and consistent with the reported N–N bond lengths in $(\text{N}_2)^{3-}$ -rare-earth metal complexes (1.36–1.41 Å).^{10b,d} Because of the more negative charge on the

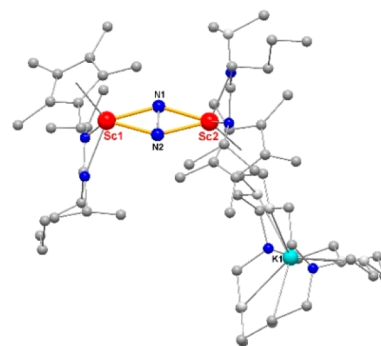


Figure 1. Molecular structure of **3** (ball-and-stick representation). Hydrogen atoms have been omitted for clarity. Selected bond lengths [Å] and angles [deg]: N1–N2 1.3963(16), Sc1–N1 2.0680(12), Sc1–N2 2.0415(12), Sc2–N1 2.0673(12), Sc2–N2 2.0475(12); N1–Sc1–N2 39.72(4), N1–Sc2–N2 39.67(4).

dinitrogen ligand, the average Sc–N(N_2) distance (2.056 Å) in **3** is significantly shorter than that in **2** (2.134 Å). In the Raman spectrum of **3**, an absorption at 975 cm^{-1} indicative of a $(\text{N}_2)^{3-}$ radical was found.¹² Furthermore, **3** has an EPR signal with a g value of 2.0051 (Figure S6), which is in line with the reported values (2.0038 for Y^{10b} and 2.0025 for La^{10d}). The multiline pattern of this spectrum is consistent with the simulated spectrum, which is split by two ^{45}Sc ($I = 7/2$) atoms and two ^{14}N ($I = 1$) atoms. To the best of our knowledge, **3** represents the first scandium complex with a $(\text{N}_2)^{3-}$ ligand. Density functional theory (DFT) studies further confirmed the structure of **3**. The singly occupied molecular orbital (SOMO) of **3** (Figure S35) is the essentially unperturbed π^* orbital of N_2 perpendicular to the Sc_2N_2 plane (see the Supporting Information (SI) for details).

The reaction of **3** with carbon-based electrophiles was explored. When MeOTf was added, functionalization of the $(\text{N}_2)^{3-}$ unit occurred smoothly to give complex **4** in 43% isolated yield along with the regeneration of **2** in 55% yield (Scheme 2e). The yield of **4** could be improved by adding potassium and MeOTf several times to the reaction mixture (Scheme 2f; see the SI for details). The molecular structure of **4** reveals a $(\text{N}_2\text{Me}_2)^{2-}$ -bridged discandium complex (Figure 2). The dihedral angle between the Sc1–N1–N2 and Sc2–N1–N2 planes is $41.09(4)^\circ$, which indicates that the Sc_2N_2 unit is not coplanar. The length of the N1–N2 bond in **4**

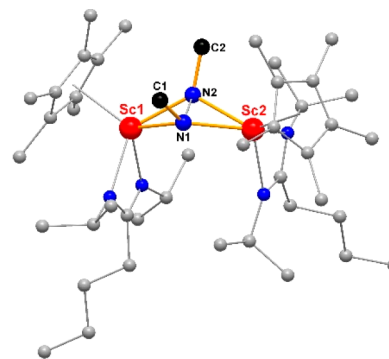
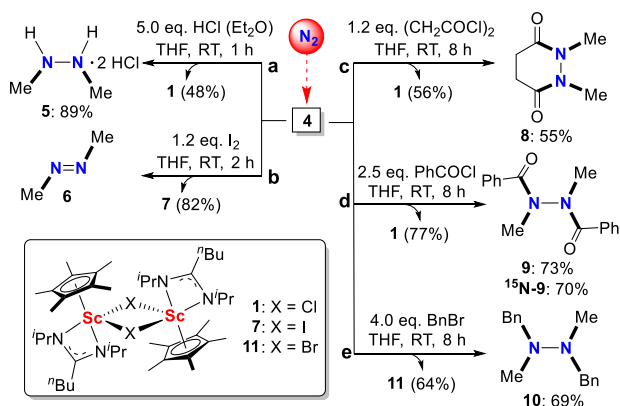


Figure 2. Molecular structure of **4** (ball-and-stick representation). Hydrogen atoms have been omitted for clarity. Selected bond lengths [Å] and angles [deg]: N1–N2 1.5044(16), C1–N1 1.4718(18), C2–N2 1.4744(18), Sc1–N1 2.2131(11), Sc1–N2 2.1292(11); N1–Sc1–N2 40.48(4), N1–Sc2–N2 40.38(4).

(1.5044(16) Å) is obviously longer than the corresponding N1–N2 bond in **3** (1.3963(16) Å) and is similar to the N–N distances observed in $(\text{N}_2\text{H}_2)^{2-}$ complexes derived from N_2 .^{10e,15} In the ^{15}N NMR spectrum of ^{15}N -**4**, a δ value of -231.04 ppm is observed for the $(^{15}\text{N}_2\text{Me}_2)^{2-}$ group, which is shifted significantly upfield in comparison with that of **2**. As far as we are aware, this methylation represents the first example of the use of a $(\text{N}_2)^{3-}$ -metal complex to construct C–N bonds using N_2 as the nitrogen source, and **4** is also the first $(\text{N}_2\text{Me}_2)^{2-}$ complex derived from the N_2 molecule. In contrast to **3**, complex **2** was stable toward MeOTf.

Further transformation of the $(\text{N}_2\text{Me}_2)^{2-}$ -bridged discandium complex **4**, whose $(\text{N}_2\text{Me}_2)^{2-}$ unit was directly derived from N_2 , was investigated (Scheme 3). Protonolysis of **4** with

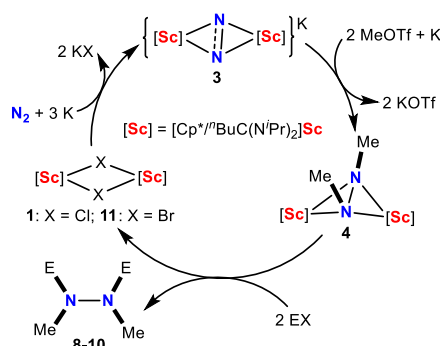
Scheme 3. Representative Reactions of **4** with HCl, I_2 , $(\text{CH}_2\text{COCl})_2$, PhCOCl, and BnBr



an Et_2O solution of anhydrous HCl was carried out, affording 1,2-dimethylhydrazine (**5**) in 89% yield (Scheme 3a). When **4** was treated with iodine, the $(\text{N}_2\text{Me}_2)^{2-}$ unit was oxidized to generate azomethane **6** accompanied by the formation of **7** (Scheme 3b). More remarkably, the $(\text{N}_2\text{Me}_2)^{2-}$ unit could be functionalized by reaction with electrophiles via further formation of C–N bonds. Thus, treatment of **4** with acyl chlorides and benzyl bromide led to the formation of the corresponding tetrasubstituted hydrazine derivatives **8–10** (Scheme 3c–e) with the regeneration of **1** or **11**. Besides, ^{15}N -labeled ^{15}N -**9** (^{15}N NMR: $\delta = -240.63$ ppm) was obtained in 70% isolated yield from ^{15}N -**4** (Scheme 3d), providing an efficient route to access ^{15}N -labeled hydrazine derivatives. The generation of four C–N bonds on the N–N skeleton and ^{15}N -labeled hydrazine derivatives directly from N_2 or $^{15}\text{N}_2$ is unprecedented (Scheme 3c–e).

As analogues of **1**, complexes **7** and **11** (Scheme 3) could react with potassium under N_2 to provide **3**. Thus, as shown in Scheme 4, a synthetic cycle could be realized for scandium-mediated conversion of N_2 , MeOTf, and electrophiles to hydrazine derivatives. The cycle includes three main steps: (i) reduction of the halogen-bridged discandium complex under N_2 , leading to the formation of the $(\text{N}_2)^{3-}$ -bridged discandium complex; (ii) treatment of the $(\text{N}_2)^{3-}$ complex with MeOTf, affording the $(\text{N}_2\text{Me}_2)^{2-}$ -bridged discandium complex; and (iii) further reaction of the $(\text{N}_2\text{Me}_2)^{2-}$ complex with a carbon-based electrophile (EX) to produce a hydrazine derivative and regenerate the halogen-bridged discandium complex. To test the efficiency of this cycle, a one-pot reaction via sequential addition of potassium, MeOTf, and PhCOCl to a THF

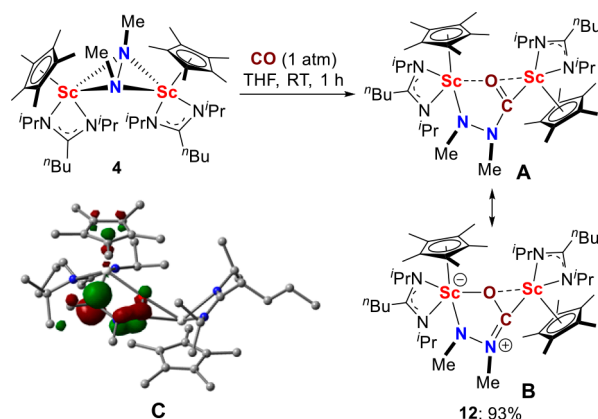
Scheme 4. Synthetic Cycle Affording Hydrazine Derivatives Using N_2 as the Nitrogen Source



solution of **1** was carried out, providing the N-containing compound **9** in 47% isolated yield along with regeneration of **1** in 57% yield (see the SI for details).

Because of the abundance of carbon monoxide (CO), the direct combination of N_2 and CO should be an attractive way to construct C–N bonds.^{2c,5} When CO was bubbled into a THF solution of **4** (Scheme 5), the new dinuclear scandium

Scheme 5. Reaction of **4** with CO



complex **12**, formed via 1,1-insertion of one CO molecule into a Sc–N bond in **4**, was obtained in 93% isolated yield. The structure of **12** was confirmed by X-ray diffraction analysis (Figure 3). The CO unit is bonded with a scandium atom in an

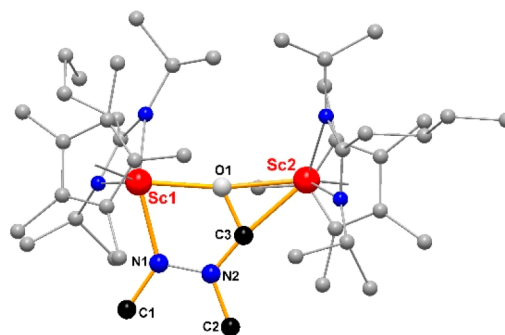


Figure 3. Molecular structure of **12** (ball-and-stick representation). Hydrogen atoms have been omitted for clarity. Selected bond lengths [Å] and angles [deg]: N1–N2 1.399(3), C3–N2 1.303(3), C3–O1 1.367(3), Sc1–O1 2.1633(17), Sc2–O1 2.1998(17), Sc2–C3 2.166(3); N2–C3–O1 114.3(2), O1–Sc1–N1 72.65(7).

η^2 fashion, which is analogous to the previous reports of CO insertion into An–N (An = Th, U)¹⁶ and Sc–B¹⁷ bonds. In **12**, the C3–N2 and C3–O1 distances are 1.303(3) and 1.367(3) Å, which are outside the ranges of standard lengths of C–N single bonds (1.366–1.380 Å) and C=O double bonds (1.212–1.225 Å) in organic amides, respectively.¹⁶ In order to understand the bonding mode in **12**, DFT calculations were carried out, and the optimized structural parameters agree well with the solid-state structure (see the SI for details). The HOMO (Scheme 5C) is mainly composed of p orbitals of the N1, N2, and C3 atoms. The Wiberg bond indexes of the C3–N2 and C3–O1 bonds are 1.41 and 1.11, in line with double-bond character of the C3–N2 bond and single-bond character of the C3–O1 bond, respectively. Hence, **12** is best described as two resonance forms (A and B in Scheme 5) with a greater contribution from B.

In summary, we have demonstrated a synthetic cycle of scandium-mediated conversion of N₂ and ¹⁵N₂ to hydrazine derivatives via the formation of C–N bonds in (N₂)³⁻ and (N₂Me₂)²⁻–scandium intermediates. This process represents the first rare-earth metal-promoted incorporation of N₂ into organic compounds and provides a useful method for the preparation of ¹⁵N-labeled hydrazine derivatives. Moreover, upon addition of CO to this (N₂Me₂)²⁻–scandium complex, the assembly of a C–N bond from CO and N₂ was observed.

■ ASSOCIATED CONTENT

Supporting Information

The Supporting Information is available free of charge on the ACS Publications website at DOI: 10.1021/jacs.9b04293.

Experimental details; X-ray data for **1–4**, **7**, **11**, and **12**; NMR spectra of new compounds; EPR spectra of **3**; and Raman spectra of **2**, ¹⁵N-**2**, **3**, ¹⁵N-**3**, **4**, and ¹⁵N-**4** (PDF)

Crystallographic data for **1–4**, **7**, **11**, and **12** (CIF)

■ AUTHOR INFORMATION

Corresponding Authors

*wx_zhang@pku.edu.cn

*zfxi@pku.edu.cn

ORCID

Ze-Jie Lv: 0000-0003-1994-8400

Zhe Huang: 0000-0002-9201-9491

Wen-Xiong Zhang: 0000-0003-0744-2832

Zhenfeng Xi: 0000-0003-1124-5380

Notes

The authors declare no competing financial interest.

■ ACKNOWLEDGMENTS

This work was supported by the National Natural Science Foundation of China (21725201, 21890721, and 21690061), Peking University, Beijing National Laboratory for Molecular Sciences (BNLMS), and the High-Performance Computing Platform of Peking University. The authors thank Prof. S.-D. Jiang and Mr. Z. Liu for carrying out the EPR measurement and data analysis.

■ REFERENCES

- (1) For selected reviews of dinitrogen activation promoted by transition metal complexes, see: (a) Schrock, R. R. Catalytic Reduction of Dinitrogen to Ammonia at a Single Molybdenum Center. *Acc. Chem. Res.* **2005**, *38*, 955–962. (b) Jia, H.-P.; Quadrelli, E. A. Mechanistic Aspects of Dinitrogen Cleavage and Hydrogenation to Produce Ammonia in Catalysis and Organometallic Chemistry: Relevance of Metal Hydride Bonds and Dihydrogen. *Chem. Soc. Rev.* **2014**, *43*, 547–564. (c) Nishibayashi, Y. Recent Progress in Transition-Metal-Catalyzed Reduction of Molecular Dinitrogen under Ambient Reaction Conditions. *Inorg. Chem.* **2015**, *54*, 9234–9247. (d) Bezdek, M. J.; Chirik, P. J. Expanding Boundaries: N₂ Cleavage and Functionalization beyond Early Transition Metals. *Angew. Chem., Int. Ed.* **2016**, *55*, 7892–7896. (e) Burford, R. J.; Fryzuk, M. D. Examining the Relationship between Coordination Mode and Reactivity of Dinitrogen. *Nat. Rev. Chem.* **2017**, *1*, 0026. (f) Li, J.; Yin, J.; Yu, C.; Zhang, W.-X.; Xi, Z. Direct Transformation of N₂ to N-Containing Organic Compounds. *Huaxue Xuebao* **2017**, *75*, 733–743.
- (2) (a) Shima, T.; Hu, S.; Luo, G.; Kang, X.; Luo, Y.; Hou, Z. Dinitrogen Cleavage and Hydrogenation by a Trinuclear Titanium Polyhydride Complex. *Science* **2013**, *340*, 1549–1552. (b) Guru, M. M.; Shima, T.; Hou, Z. Conversion of Dinitrogen to Nitriles at a Multinuclear Titanium Framework. *Angew. Chem., Int. Ed.* **2016**, *55*, 12316–12320. (c) Knobloch, D. J.; Lobkovsky, E.; Chirik, P. J. Dinitrogen Cleavage and Functionalization by Carbon Monoxide Promoted by a Hafnium Complex. *Nat. Chem.* **2010**, *2*, 30–35. (d) Semproni, S. P.; Chirik, P. J. Synthesis of a Base-Free Hafnium Nitride from N₂ Cleavage: A Versatile Platform for Dinitrogen Functionalization. *J. Am. Chem. Soc.* **2013**, *135*, 11373–11383. (e) Semproni, S. P.; Chirik, P. J. Activation of Dinitrogen-Derived Hafnium Nitrides for Nucleophilic N–C Bond Formation with a Terminal Isocyanate. *Angew. Chem.* **2013**, *125*, 13203–13207.
- (3) (a) Ishida, Y.; Kawaguchi, H. Nitrogen Atom Transfer from a Dinitrogen-Derived Vanadium Nitride Complex to Carbon Monoxide and Isocyanide. *J. Am. Chem. Soc.* **2014**, *136*, 16990–16993. (b) Figueroa, J. S.; Piro, N. A.; Clough, C. R.; Cummins, C. C. A Nitridoniobium(V) Reagent That Effects Acid Chloride to Organic Nitrile Conversion: Synthesis via Heterodinuclear (Nb/Mo) Dinitrogen Cleavage, Mechanistic Insights, and Recycling. *J. Am. Chem. Soc.* **2006**, *128*, 940–950. (c) Akagi, F.; Matsuo, T.; Kawaguchi, H. Dinitrogen Cleavage by a Diniobium Tetrahydride Complex: Formation of a Nitride and Its Conversion into Imide Species. *Angew. Chem., Int. Ed.* **2007**, *46*, 8778–8781.
- (4) (a) Curley, J. J.; Sceats, E. L.; Cummins, C. C. A Cycle for Organic Nitrile Synthesis via Dinitrogen Cleavage. *J. Am. Chem. Soc.* **2006**, *128*, 14036–14037. (b) Keane, A. J.; Farrell, W. S.; Yonke, B. L.; Zavalij, P. Y.; Sita, L. R. Metal-Mediated Production of Isocyanates, R₃EN=C=O from Dinitrogen, Carbon Dioxide, and R₃ECl. *Angew. Chem., Int. Ed.* **2015**, *54*, 10220–10224. (c) Klopsch, I.; Finger, M.; Würtele, C.; Milde, B.; Werz, D. B.; Schneider, S. Dinitrogen Splitting and Functionalization in the Coordination Sphere of Rhenium. *J. Am. Chem. Soc.* **2014**, *136*, 6881–6883. (d) Klopsch, I.; Kinauer, M.; Finger, M.; Würtele, C.; Schneider, S. Conversion of Dinitrogen into Acetonitrile under Ambient Conditions. *Angew. Chem., Int. Ed.* **2016**, *55*, 4786–4789. (e) Schendzielorz, F.; Finger, M.; Abbenseth, J.; Würtele, C.; Krewald, V.; Schneider, S. Metal-Ligand Cooperative Synthesis of Benzonitrile by Electrochemical Reduction and Photolytic Splitting of Dinitrogen. *Angew. Chem., Int. Ed.* **2019**, *58*, 830–834. (f) Betley, T. A.; Peters, J. C. Dinitrogen Chemistry from Trigonal Coordinated Iron and Cobalt Platforms. *J. Am. Chem. Soc.* **2003**, *125*, 10782–10783. (g) MacLeod, K. C.; Menges, F. S.; McWilliams, S. F.; Craig, S. M.; Mercado, B. Q.; Johnson, M. A.; Holland, P. L. Alkali-Controlled C–H Cleavage or N–C Bond Formation by N₂-Derived Iron Nitrides and Imides. *J. Am. Chem. Soc.* **2016**, *138*, 11185–11191.
- (5) (a) Falcone, M.; Chatelain, L.; Scopelliti, R.; Zivkovic, I.; Mazzanti, M. Nitrogen Reduction and Functionalization by a Multimetallic Uranium Nitride Complex. *Nature* **2017**, *547*, 332–335. (b) Falcone, M.; Barluzzi, L.; Andrez, J.; Fadaei Tirani, F.; Zivkovic, I.; Fabrizio, A.; Corminboeuf, C.; Severin, K.; Mazzanti, M. The Role of Bridging Ligands in Dinitrogen Reduction and

Functionalization by Uranium Multimetallic Complexes. *Nat. Chem.* **2019**, *11*, 154–160.

(6) Ragnarsson, U. Synthetic Methodology for Alkyl Substituted Hydrazines. *Chem. Soc. Rev.* **2001**, *30*, 205–220.

(7) (a) Pickett, C. J.; Leigh, G. J. Towards a Nitrogen-Fixing Cycle: Electrochemical Reduction of a Hydrazido-Complex of Molybdenum(IV) under N_2 to Yield the Dialkylhydrazine and a Molybdenum(0) Dinitrogen Complex. *J. Chem. Soc., Chem. Commun.* **1981**, 1033–1035. (b) Hidai, M.; Mizobe, Y. Recent Advances in the Chemistry of Dinitrogen Complexes. *Chem. Rev.* **1995**, *95*, 1115–1133. (c) Hidai, M. Chemical Nitrogen Fixation by Molybdenum and Tungsten Complexes. *Coord. Chem. Rev.* **1999**, *185–186*, 99–108. (d) Bernskoetter, W. H.; Lobkovsky, E.; Chirik, P. J. Nitrogen–Carbon Bond Formation from N_2 and CO_2 Promoted by a Hafnocene Dinitrogen Complex Yields a Substituted Hydrazine. *Angew. Chem., Int. Ed.* **2007**, *46*, 2858–2861. (e) Knobloch, D. J.; Toomey, H. E.; Chirik, P. J. Carboxylation of an *ansa*-Zirconocene Dinitrogen Complex: Regio-specific Hydrazine Synthesis from N_2 and CO_2 . *J. Am. Chem. Soc.* **2008**, *130*, 4248–4249. (f) Knobloch, D. J.; Benito-Garagorri, D.; Bernskoetter, W. H.; Keresztes, I.; Lobkovsky, E.; Toomey, H.; Chirik, P. J. Addition of Methyl Triflate to a Hafnocene Dinitrogen Complex: Stepwise N_2 Methylation and Conversion to a Hafnocene Hydrazonato Compound. *J. Am. Chem. Soc.* **2009**, *131*, 14903–14912. (g) Nakanishi, Y.; Ishida, Y.; Kawaguchi, H. Nitrogen–Carbon Bond Formation by Reactions of a Titanium–Potassium Dinitrogen Complex with Carbon Dioxide, *tert*-Butyl Isocyanate, and Phenylallene. *Angew. Chem., Int. Ed.* **2017**, *56*, 9193–9197.

(8) (a) Fryzuk, M. D.; Johnson, S. A.; Patrick, B. O.; Albinati, A.; Mason, S. A.; Koetzle, T. F. New Mode of Coordination for the Dinitrogen Ligand: Formation, Bonding, and Reactivity of a Tantalum Complex with a Bridging N_2 Unit That Is Both Side-On and End-On. *J. Am. Chem. Soc.* **2001**, *123*, 3960–3973. (b) Morello, L.; Love, J. B.; Patrick, B. O.; Fryzuk, M. D. Carbon–Nitrogen Bond Formation via the Reaction of Terminal Alkynes with a Dinuclear Side-on Dinitrogen Complex. *J. Am. Chem. Soc.* **2004**, *126*, 9480–9481. (c) Bernskoetter, W. H.; Olmos, A. V.; Pool, J. A.; Lobkovsky, E.; Chirik, P. J. N–C Bond Formation Promoted by a Hafnocene Dinitrogen Complex: Comparison of Zirconium and Hafnium Congeners. *J. Am. Chem. Soc.* **2006**, *128*, 10696–10697. (d) Hirotsu, M.; Fontaine, P. P.; Zavalij, P. Y.; Sita, L. R. Extreme $N\equiv N$ Bond Elongation and Facile N-Atom Functionalization Reactions within two Structurally Versatile New Families of Group 4 Bimetallic “Side-on-Bridged” Dinitrogen Complexes for Zirconium and Hafnium. *J. Am. Chem. Soc.* **2007**, *129*, 12690–12692. (e) Ballmann, J.; Yeo, A.; Patrick, B. O.; Fryzuk, M. D. Carbon–Nitrogen Bond Formation by the Reaction of 1,2-Cumulenes with a Ditanalium Complex Containing Side-on- and End-on-Bound Dinitrogen. *Angew. Chem., Int. Ed.* **2011**, *50*, 507–510.

(9) For selected reports on $(N_2)^{2-}$ –rare-earth metal complexes, see: (a) Evans, W. J.; Ulibarri, T. A.; Ziller, J. W. Isolation and X-ray Crystal Structure of the First Dinitrogen Complex of an f-Element Metal, $[(C_5Me_5)_2Sm]_2N_2$. *J. Am. Chem. Soc.* **1988**, *110*, 6877–6879. (b) Evans, W. J.; Lee, D. S. Early Developments in Lanthanide-Based Dinitrogen Reduction Chemistry. *Can. J. Chem.* **2005**, *83*, 375–384. (c) Evans, W. J.; Lee, D. S.; Ziller, J. W.; Kaltsoyannis, N. Trivalent $[(C_5Me_5)_2(THF)Ln]_2(\mu-\eta^2-\eta^2-N_2)$ Complexes as Reducing Agents Including the Reductive Homologation of CO to a Ketene Carboxylate, $(\mu-\eta^4-O_2C-C\equiv C=O)^{2-}$. *J. Am. Chem. Soc.* **2006**, *128*, 14176–14184. (d) Cheng, J.; Takats, J.; Ferguson, M. J.; McDonald, R. Heteroleptic Tm(II) Complexes: One more Success for Trofimenko’s Scorpionates. *J. Am. Chem. Soc.* **2008**, *130*, 1544–1545. (e) Jaroschik, F.; Momin, A.; Nief, F.; Le Goff, X.-F.; Deacon, G. B.; Junk, P. C. Dinitrogen Reduction and C–H Activation by the Divalent Organoneodymium Complex $[(C_5H_2fBu_3)_2Nd(\mu-I)K([18]-crown-6)]$. *Angew. Chem., Int. Ed.* **2009**, *48*, 1117–1121. (f) Demir, S.; Lorenz, S. E.; Fang, M.; Furche, F.; Meyer, G.; Ziller, J. W.; Evans, W. J. Synthesis, Structure, and Density Functional Theory Analysis of a Scandium Dinitrogen Complex, $[(C_5Me_4H)_2Sc]_2(\mu-\eta^2-\eta^2-N_2)$. *J. Am. Chem. Soc.* **2010**, *132*, 11151–11158. (g) Mueller, T. J.; Fieser,

M. E.; Ziller, J. W.; Evans, W. J. $(C_5Me_4H)^{1-}$ -Based Reduction of Dinitrogen by the Mixed Ligand Tris(polyalkylcyclopentadienyl) Lutetium and Yttrium Complexes, $(C_5Me_5)_{3-x}(C_5Me_4H)_xLn$. *Chem. Sci.* **2011**, *2*, 1992–1996. (h) Fieser, M. E.; Bates, J. E.; Ziller, J. W.; Furche, F.; Evans, W. J. Dinitrogen Reduction via Photochemical Activation of Heteroleptic Tris(cyclopentadienyl) Rare-Earth Complexes. *J. Am. Chem. Soc.* **2013**, *135*, 3804–3807.

(10) For selected reports on $(N_2)^{3-}$ and other rare-earth metal dinitrogen complexes, see: (a) Dubé, T.; Conoci, S.; Gambarotta, S.; Yap, G. P. A.; Vasapollo, G. Tetrametallic Reduction of Dinitrogen: Formation of a Tetranuclear Samarium Dinitrogen Complex. *Angew. Chem., Int. Ed.* **1999**, *38*, 3657–3659. (b) Evans, W. J.; Fang, M.; Zucchi, G.; Furche, F.; Ziller, J. W.; Hoekstra, R. M.; Zink, J. I. Isolation of Dysprosium and Yttrium Complexes of a Three-Electron Reduction Product in the Activation of Dinitrogen, the $(N_2)^{3-}$ Radical. *J. Am. Chem. Soc.* **2009**, *131*, 11195–11202. (c) Evans, W. J.; Fang, M.; Bates, J. E.; Furche, F.; Ziller, J. W.; Kiesz, M. D.; Zink, J. I. Isolation of a Radical Dianion of Nitrogen Oxide $(NO)^{2-}$. *Nat. Chem.* **2010**, *2*, 644–647. (d) Fang, M.; Bates, J. E.; Lorenz, S. E.; Lee, D. S.; Rego, D. B.; Ziller, J. W.; Furche, F.; Evans, W. J. $(N_2)^{3-}$ Radical Chemistry via Trivalent Lanthanide Salt/Alkali Metal Reduction of Dinitrogen: New Syntheses and Examples of $(N_2)^{2-}$ and $(N_2)^{3-}$ Complexes and Density Functional Theory Comparisons of Closed Shell Sc^{3+} , Y^{3+} , Lu^{3+} versus $4f^9 Dy^{3+}$. *Inorg. Chem.* **2011**, *50*, 1459–1469. (e) Fang, M.; Lee, D. S.; Ziller, J. W.; Doedens, R. J.; Bates, J. E.; Furche, F.; Evans, W. J. Synthesis of the $(N_2)^{3-}$ Radical from Y^{2+} and Its Protonolysis Reactivity to Form $(N_2H_2)^{2-}$ via the $Y[N(SiMe_3)_2]_3/KC_8$ Reduction System. *J. Am. Chem. Soc.* **2011**, *133*, 3784–3787. (f) Rinehart, J. D.; Fang, M.; Evans, W. J.; Long, J. R. Strong Exchange and Magnetic Blocking in N_2^{3-} -Radical-Bridged Lanthanide Complexes. *Nat. Chem.* **2011**, *3*, 538–542. (g) Meihaus, M. R.; Corbey, J. F.; Fang, M.; Ziller, J. W.; Long, J. R.; Evans, W. J. Influence of an Inner-Sphere K^+ Ion on the Magnetic Behavior of N_2^{3-} Radical-Bridged Dilanthanide Complexes Isolated Using an External Magnetic Field. *Inorg. Chem.* **2014**, *53*, 3099–3107. (h) Demir, S.; Gonzalez, M. I.; Darago, L. E.; Evans, W. J.; Long, J. R. Giant Coercivity and High Magnetic Blocking Temperatures for N_2^{3-} Radical-Bridged Dilanthanide Complexes upon Ligand Dissociation. *Nat. Commun.* **2017**, *8*, 2144.

(11) Walter, M. D. Recent Advances in Transition Metal-Catalyzed Dinitrogen Activation. *Adv. Organomet. Chem.* **2016**, *65*, 261–377.

(12) Tanabe, Y. Group 3 Transition Metal, Lanthanide, and Actinide–Dinitrogen Complexes. In *Transition Metal–Dinitrogen Complexes*; Nishibayashi, Y., Ed.; Wiley-VCH: Weinheim, Germany, 2019; Chapter 9, pp 441–474.

(13) Fieser, M. E.; Woen, D. H.; Corbey, J. F.; Mueller, T. J.; Ziller, J. W.; Evans, W. J. Raman Spectroscopy of the N–N Bond in Rare Earth Dinitrogen Complexes. *Dalton Trans.* **2016**, *45*, 14634–14644.

(14) Woen, D. H.; Chen, G. P.; Ziller, J. W.; Boyle, T. J.; Furche, F.; Evans, W. J. End-on Bridging Dinitrogen Complex of Scandium. *J. Am. Chem. Soc.* **2017**, *139*, 14861–14864.

(15) (a) Pool, J. A.; Lobkovsky, E.; Chirik, P. J. Hydrogenation and Cleavage of Dinitrogen to Ammonia with a Zirconium Complex. *Nature* **2004**, *427*, 527–530. (b) Bernskoetter, W. H.; Olmos, A. V.; Lobkovsky, E.; Chirik, P. J. N_2 Hydrogenation Promoted by a Side-on Bound Hafnocene Dinitrogen Complex. *Organometallics* **2006**, *25*, 1021–1027. (c) Morello, L.; João Ferreira, M.; Patrick, B. O.; Fryzuk, M. D. Side-on Bound Dinitrogen Complex of Zirconium Supported by a P_2N_2 Macrocyclic Ligand. *Inorg. Chem.* **2008**, *47*, 1319–1323.

(16) Fagan, P. J.; Manriquez, J. M.; Vollmer, S. H.; Day, C. S.; Day, V. W.; Marks, T. J. Insertion of Carbon Monoxide into Metal–Nitrogen Bonds. Synthesis, Chemistry, Structures, and Structural Dynamics of Bis(pentamethylcyclopentadienyl) Organoactinide Dialkylamides and η^2 -Carbamoyls. *J. Am. Chem. Soc.* **1981**, *103*, 2206–2020.

(17) Wang, B.; Kang, X.; Nishiura, M.; Luo, Y.; Hou, Z. Isolation, Structure and Reactivity of a Scandium Boryl Oxycarbene Complex. *Chem. Sci.* **2016**, *7*, 803–809.